Proposal and Characterization of Ring Resonator with Sharp U-Turns Using an SOI-Based Photonic Crystal Waveguide

Yasuhisa Omura, Yukio Iida, Fumio Urakawa, and Yoshifumi Ogawa

Abstract—We propose and experimentally demonstrate a ring resonator with sharp U-turns fabricated on a silicon-on-insulator (SOI) substrate; the resonator was designed as a key part of an optical, dynamic data storage device. We discuss the optical properties of the fabricated ring resonator from the viewpoint of equi-frequency-contour behavior in a dispersion space. We successfully characterize its optical characteristics on the basis of photonic crystal physics. It is suggested that the photonic ring resonator will be applicable to optical, dynamic memory devices for optical communication systems.

Index words—SOI, photonic crystal, ring resonator, FDTD simulations

I. INTRODUCTION

Two-dimensional (2-D) photonic crystal have high potential in terms of light-beam control capability and so have attracted much attention. Since 2-D photonic crystals have a wide variety of photonic band structures, it is expected that the propagation of light can be manipulated in sophisticated way by using 2-D photonic crystals [1-17]. Any light wave mode whose frequency is in the photonic band gap (PBG) basically can't propagate through a photonic crystal. However, the insertion of "defects" allows the photonic crystal to work as a waveguide or a resonator [4]. Photonic crystal waveguides using such defect modes have been widely

studied from the viewpoint of application to sharp-bend waveguides, frequency filters, and photonic switching devices [5-7]. In addition, in some cases, the photonic crystal imposes specific restrictions on light wave propagation even beyond the PBG; super-prism, self-collimation, and super-lens are typical phenomena [8-17]. These phenomena suggest higher potential applications of the photonic crystal to information processing because they are related to the photonic band structures implemented.

For photonic crystals built on dielectric slabs, a triangular lattice of air holes is often considered; this yields a wider omni-directional TE-PBG than the square array [5, 18]. It has been considered that photonic crystal should not use square lattices when forming sharp waveguide bends. Recently, however, we found through finite-difference time-domain (FDTD) simulations of an original photonic crystal that low-loss transmission was possible in a frequency range outside the PBG in the longitudinal and transverse directions, except for the low-loss transmission frequency in the oblique direction [4]. Based on this we proposed a possible structure for a ring resonator with sharp U-turns that offered relatively high Q-values [4]. Our simulations also showed that the resonant frequency was about 200 THz (infra-red range). For example, for a resonance frequency of 211 THz, the full width at half maximum (FWHM) of the tuning curve was 2.1 THz. This corresponds to Q=100, where Q is the quality factor of the resonator. We also performed 30,000-FDTD time-step simulations; this time step corresponds to a resonant frequency of 110 cycles and the resolution of the Fourier transform become 1.9 THz. As a result, the Q-value obtained from the tuning curve approached 100,

even if the resonator's Q was very high. Based on these facts, our expectation was that a resonator with sharp U-turns should have a Q-value larger than 100.
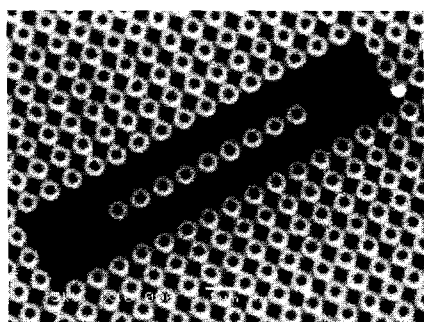
In this paper, we experimentally demonstrate a ring resonator with sharp U-turns fabricated on a silicon-on-insulator (SOI) substrate, and discuss its optical properties from the viewpoint of equi-frequency-contour behavior in a dispersion space [19, 20]. It is shown that 2-D photonic crystals with square lattices are suitable for forming sharp waveguide bends in practice when the photonic crystal is well tempered in the dispersion space.

II. EXPERIMENTAL RESULTS

Fig. 1(a) shows the ring resonator introduced here; we target infrared light wave transmission in a Si-based photonic crystal from the viewpoint of connection to conventional optical waveguides and Si-LSI's. Figure 1(b) shows an SEM view of the ring resonator fabricated on an SOI substrate. Air-hole patterns were exposed by the electron-beam direct writing technique and the air holes were realized by the dry-etching technique. An infrared-TV-camera view of the ring resonator is shown in Fig. 2(a); a ring resonator can be seen, but it is dark in
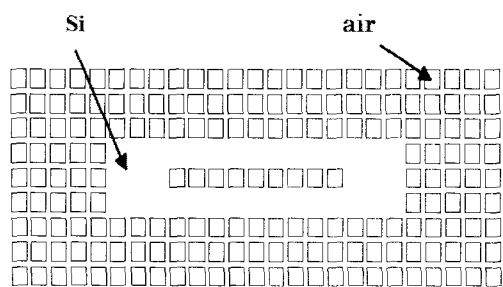
(a) Visible light is injected into the ring.

(b) Infra-red light (1550-nm wavelength) is injected into the ring from its wide side.

Fig. 2. Infrared TV camera view of photonic crystal with illumination of the ring resonator under.

the photonic crystal field. Fig. 2(b) shows the same view when a 1550-nm wavelength (193 THz) laser light is injected (denoted by an arrow) into the photonic crystal through a single mode fiber with a focus lens; the light enters from the wider side of the ring resonator. We fabricated many ring resonators on SOI substrates with different SOI layer thickness and different air-hole sizes. The resonator brightened with both 1550-nm (193 THz) and 1310-nm (229 THz) laser light injection was chosen. The lattice constant is about 800 nm, the air-holes are about 350-nm square, the SOI layer is about 300 nm thick, and the buried oxide layer is 1 μm thick. We can observe strong brightness in the ring region at the center of the photonic crystal.

With illumination from the narrow side of the ring resonator, strong brightness is also observed for wavelengths of both 1550 nm and 1310 nm. The spectra of the resonator field were obtained using a single-mode fiber to inject 1550-nm wave laser light. The source spectra of the 1550-nm wave laser are shown in Fig. 3(a). We found that the observed spectra of the light wave output by the photonic crystal with the ring shifted during the observation; over time, the observed spectrum is switched from Figs. 3(b) to 3(c), and 3(d), and more complex spectra. We think that the variation in the observed spectra corresponds to the size modulation established by the substrate-temperature change created by the strong laser beam having an energy lower than the
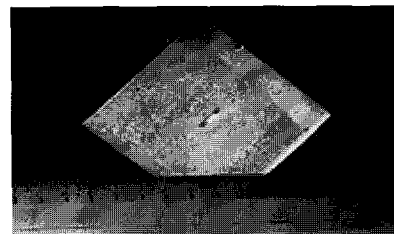

Si   air
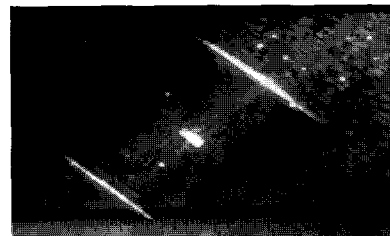
(a) Ring resonator realized in photonic crystal.

(b) SEM view of ring resonator fabricated on SOI substrate.

Fig. 1. Ring resonator with sharp U-turns formed in photonic crystal with a square lattice of square air holes.

band-gap of silicon. We note that spectra shown in Fig. 3(d) was replaced by the initial spectrum when the laser irradiation was turned off as seen in Figs. 3(e) to 3(g).

III. DISCUSSION

We simulated the optical characteristics of the fabricated ring resonator. Fig. 4 shows the finite-difference time-domain (FDTD) simulation model; FDTD simulations were carried out in the 10   m x 10   m area of the photonic crystal containing the ring resonator; the SOI layer was assumed to be 300-nm thick. The simulations did not take account of the Si substrate below the SiO$_2$ layer for simplicity. Two laser-light-illumination directions are shown in Fig. 4; A to D are the observation points for laser-light injection from the wide side of the ring resonator, while E to H are the observation points for laser-light injection from the narrow side of the ring resonator. Fig. 5 shows the band diagram of the 2-D photonic crystal calculated using the plane-wave expansion method of (289 x 289); in the electromagnetic field simulations, the thickness of slab is taken into account, and 3-D simulation results are obtained. However, we demonstrate primarily the electromagnetic field in the y-z plane because we focus
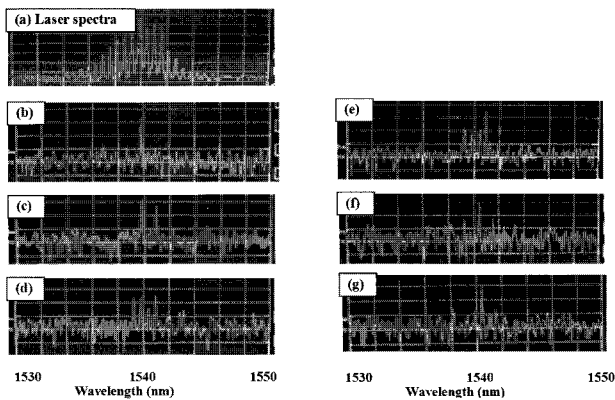
on propagation characteristics of localized waves. Since most post-fabricated air holes did have the square cross section designed (see Fig. 1(b)), we assumed that all of them had a circular cross-section with r/a =0.38, where r is the effective air hole radius. As discussed below, the simulation results suggest that the bright image shown in Fig. 2(b) can be attributed to higher energy bands; the 1550-nm wave corresponds to the normalized angular frequency $(\omega a2\pi c)$ of 0.5 and the 1310-nm wave to the normalized angular frequency $(\omega a2\pi c)$ of 0.55 in Fig. 5. From the band diagram, we can see that the 1550-nm wave (193 THz) can propagate along the Γ-X axis in the present 2-D photonic crystal, while the 1310-nm wave (229 THz) can propagate along its ΓM axis.
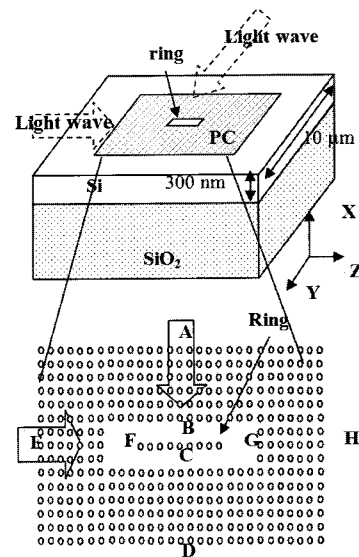

Fig. 4. FDTD simulation model. Air hole radius of 320-nm, and lattice constant of 840-nm were assumed.   Letters A to H indicate the observation points.
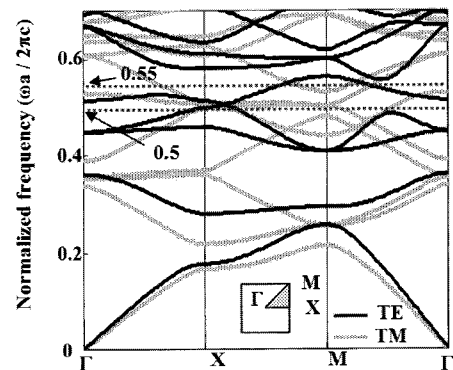

Fig. 3. Laser light spectrum and observed light spectra.
(a) is the laser source spectrum. (b), (c), and (d) are the observed spectra of resonator field picked up by single mode fiber with illumination from the narrow side of the ring. (b) was observed just after laser illumination, (c) was observed after one minute of laser illumination, and (d) was taken after 4 minutes of laser illumination. (e), (f) and (g) are also the observed spectra of resonator field picked up by single mode fiber under illumination from the narrow side of the ring. (e) was observed 5 minutes after turning off the laser illumination, (c) was observed in 9 minutes after turning off the laser illumination, and (d) was captured 11 minutes after turning off the laser illumination.

Fig. 5. Band diagram of 2-D photonic crystal without ring resonator.
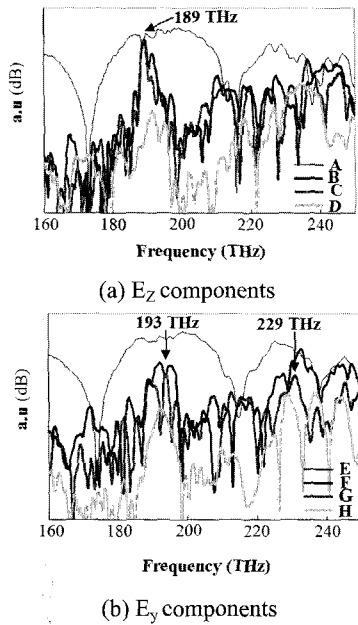
(a) E_Z components

(b) E_y components

Fig. 6. Frequency characteristics of E_Z or E_y components of the electric field observed at various points. (a) The TE mode light is injected from the wide side of the ring. (b) The TE mode light is injected from the narrow side of the ring.

The simulated frequency characteristics of the electric field (E_y component) that should be observed at points A, B, C, and D for TE-wave injection from the wide side of the ring, are shown in Fig. 6(a). Those (E_z components) at E, F, G, and H for TE-wave injection from the narrow side of ring resonator are shown in Fig. 6(b). It can be seen that two laser light waves with 1550-nm and 1310-nm wavelengths can persist in the ring resonator when TE mode light is injected from the narrow side of the ring resonator. When the TE mode light is injected from the wide side of the ring resonator, only the 1550-nm laser light wave achieves persistence. That is, the infrared-TV view shown in Fig. 2(b) is reasonable; the mechanisms are discussed later again using the band diagram. In the following, we discuss the behavior of the ring resonator from the view-point of light wave collimation in equi-frequency counters of the photonic crystal.

Fig. 7 and 9 show the simulated electric field (E_y) distributions at frequencies corresponding to 193-THz (1550-nm) wave and 229-THz (1310-nm) waves, respectively; it is assumed that the light waves are injected from the left side (the narrow side) of the photonic crystal. In both figures, (a) shows a global view of the whole photonic crystal and (b) shows an enlarged view of the ring resonator. In Fig. 7(a), it
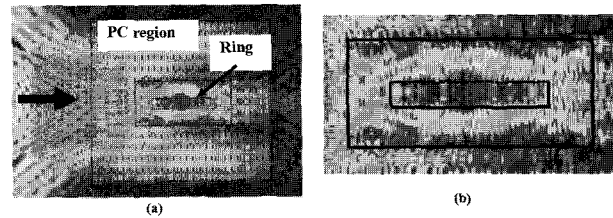

Fig. 7. Electric field (E_y) distribution at 193 THz. Light wave is injected from the narrow side of the ring. (a) Whole view of 2-D photonic crystal with the ring. (b) Enlarged view of the ring.

Fig. 8. Equi-frequency contours for the frequency $f=0.5c/a$. This corresponds to 193 THz in the ring resonator.

Fig. 9. Electric field (E_y) distribution at 229 THz. Light wave is injected from the narrow side of the ring. (a) Whole view of 2-D photonic crystal with the ring. (b) Enlarged view of the ring.
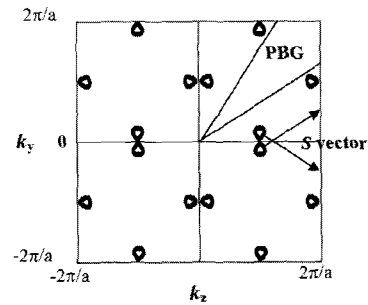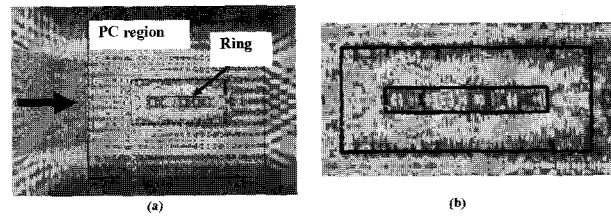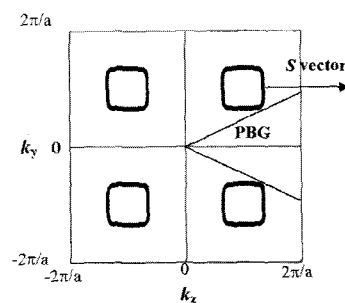

Fig. 10. Equi-frequency contours for the frequency $f=0.55c/a$. This corresponds to 229 THz in the ring resonator.

should be noted that a significant degree of incident wave reflection is seen at the interface of the silicon waveguide and the 2-D photonic crystal; this is due to mismatching of optical impedance as is discussed later [21].

From Figs. 7(b) and 9(b) we can see that the two waves (1550-nm wave and 1310-nm wave) are bound inside the ring resonator. We can see the light wave propagates in a zigzag manner in the ring because of the strong reflections yielded by the "wall" of the adjacent 2-D photonic crystal, which was predicted from the simulation results [4]. On the other hand, the power of the wave that exists the ring seems to be limited and the two waves show different behavior in the photonic crystal. To consider the behavior, we calculated the equi-frequency contours of the present photonic crystal without the ring.

Fig. 8 and 10 show simulated equi-frequency contours for the electric field distributions at 193 THz and 229 THz, respectively; in the figures, the direction having the photonic band gap in the high energy range and the S vectors of the propagating wave are described to assist the discussion. In Fig. 8 the 193 THz wave should be *significantly reflected when it is injected along the* normal direction against the left side interface of the photonic crystal because the S vector of the photonic crystal has both k_z and k_y components (Γ-M direction). Thus, we must consider that only light waves having both k_z and k_y components (a part of the light wave packet) can propagate in the photonic crystal; as seen in Fig. 7(b), the light wave is propagating along the Γ-M direction inside the ring. This suggests that light that is injected from the wide side of the ring resonator is apt to stay in the ring, which matches the results shown in Fig. 2(b) and Fig. 6(a). On the other hand, the 229 THz wave is slightly reflected when it is injected along the normal direction against the left side interface of the photonic crystal because the S vector of the photonic crystal has only the k_z component. Our assessment is that most injected light waves that have the k_z component can propagate in the photonic crystal; after arriving at the ring, the light wave also propagates in the Γ-M direction within the ring; the difference from the 193-THz wave is that the wave propagating in the Γ-M direction can pass through the surrounding photonic crystal because it has a possible mode in the Γ-M direction; this is reasonable because we can see in Fig. 9(b) that most of the power of the injected light wave is transmitted to the right side of the photonic crystal. From Fig. 6(b) we can see that the 229-THz wave can approach the ring from the narrow side of the ring resonator.

Finally, in Fig. 11,we show simulated time evolution of light waves confined in the photonic ring resonator after the incident light is switched off. In simulations, we assume that the incident light beam comes from the 'E' side of the ring resonator shown in Fig. 4. *Hx* component of light wave energy remaining around the point 'B' in Fig. 4 is shown in units of 1×10^{-24} A/m in Fig. 11(a); the frequency of major electromagnetic wave component is 220 THz. In Fig. 11(b), the *Hx* component of light wave energy in 10,000 FDTD time steps is shown in units of 1×10^{-24} A/m. In Fig. 11(c), the *Hx* component of light wave energy in 30,000 FDTD time steps is shown in units of 1×10^{-24} A/m. As seen in Fig. 11, the light wave energy remaining after the incident light beam is switched off is stationary in the photonic ring resonator. This suggests fundamentally that the photonic ring resonator works as a trap of light wave.

Our understanding of the light propagation and *confinement mechanism* of the ring resonator is supported of the equi-frequency-contour behavior in the dispersion space of the photonic crystal, and also supported by time evolution of light wave in the photonic ring resonator. The present experimental results will have a significant impact on the development of optical dynamic memory for optical circuits. When the gate component for optical memory circuit is developed [22, 23], optical dynamic memory will become possible.
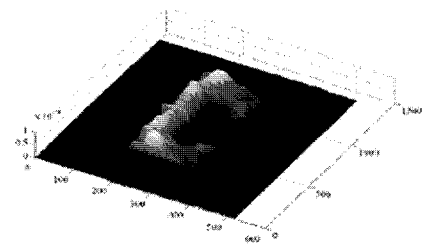
(a) Start
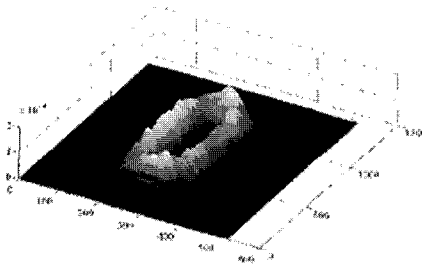
(b) 10,000 FDTD time steps
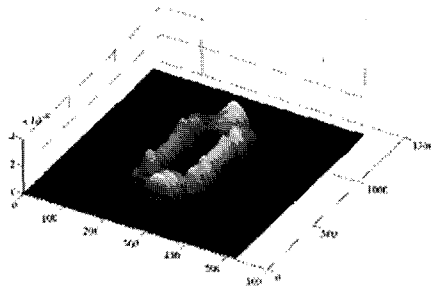
(c) 30,000 FDTD time steps

Fig. 11. Simulated time evolution of *Hx* component of light wave in photonic ring resonator.

IV. CONCLUSIONS

In this paper, we designed and fabricated a ring resonator with sharp U-turns on an SOI substrate and tested its performance. We discussed its optical properties from the viewpoint of equi-frequency-contour behavior in a dispersion space. Experimental results comprehensively agreed with the results of FDTD simulations of light wave transmission and band structure simulations for 2-D photonic crystals. The results presented herein are expected to greatly accelerate the development of practical optical dynamic memory devices for future optical circuits. When other peripheral components for optical memory circuits are developed, optical dynamic memory will play a significant role in future optical communication systems.

ACKNOWLEDGMENT

REFERENCES

[1] J. D. Joannopoulos, R. D. Meade, and J. N. Winn, "Photnic Crystals -Molding the Flow of Light," *Princeton University Press*, Princeton, NJ, 1995.

[2] K. Sakoda, "Optical Properties of Photonic crystals," *Springer*, New York, 2001.

[3] E. Yablonovitch, "Inhibited Spontaneous Emission in Solid-State Physics and Electronics," *Phys. Rev.*

Lett., vol. 58, pp. 2059-2062 (1987).

[4] Y. Iida, Y. Omura, Y. Ogawa, T. Kinoshita, and M. Tsuji, "Ring Resonator with Sharp U-Turns Using a SOI-Based Photonic Crystal Waveguide with Normal Single-Missing-Hole-Line Defect," *Proc. Of. SPIE*, Vol. 5277, pp. 206-214, 2003.

[5] Y. Akahane, T. Asano, B. S. Song, and S. Noda, "Investigation of High-Q Channel Drop Filters Using Donor-Type Defects in Two-Dimensional Photonic Crystal Slabs," *Appl. Phys. Lett.*, Vol. 83, No. 8, pp. 1512-1514, 2003.

[6] M. Soljacic, M. Ibanescu, S. G. Johnson, Y. Fink, and J. D. Joannopoulos, "Optical Bistable Switching in Nonlinear Photonic crystals," *Phys. Rev. E*, Vol. 66, pp. 055601-4, 2002.

[7] H. Takano, Y. Akahane, T. Asano, and S. Noda, "In-Plane-Type Channel Drop Filter in a Two-Dimensional Photonic Crystal Slab," *Appl. Phys. Lett.*, Vol. 84, No. 13, pp. 2226-2228, 2004.

[8] A. I. Cabuz, E. Centeno, and D. Cassagne, "Superprism Effect in Bidimensional Rectangular Photonic Crystals," *Appl. Phys. Lett.*, Vol. 84, No. 12, pp. 2031-2033, 2004.

[9] X. Yu and S. Fan, "Bends and Splitters for Self-Collimated Beams in Photonic Crystals," *Appl. Phys. Lett.*, Vol. 83, No. 16, p. 3251-3253, 2003.

[10] H. Kosada, T. Kawashima, A. Tomita, M. Notomi, T. Tamamura, T. Sato, and S. Kawakami, "Superprism Phenomena in Photonic Crystals," *Phys. Rev. B*, Vol. 58, No. 16, p. 10096-10099, 1998.

[11] X. Hu, Y. Shen, X. Liu, R. Fu, and J. Zi, "Superlensing Effect in Liquid Surface Waves," *Phys. Rev. E*, Vol. 69, pp. 030201-4, 2004.

[12] T. Matsumoto and T. Baba, "Photonic Crystal k-Vector superprism," *J. Lightwave Technol.* Vol.22, No. 3, pp. 917-922, 2004

[13] L. Wu, M. Michael, and T. F. Krauss, "Beam Steering in Planar-Photonic Crystals: From Superprism to Supercollimator," *J. Lightwave Technol.* Vol.21, No. 2, pp. 561-566, 2003.

[14] Z. Y. Li, and L.L. Lin, "Evaluation of Lensing in Photonic Crystal Slabs Exhibiting Negative Refraction," *Phys. Rev. B*, Vol. 68, pp. 245110-7, 2004.

[15] H. Kosaka, T. Kawashima, A.Tomita, M. Notomi, T. Tamamura, T. Sato, and S. Kawakami, "Self-Collimating Phenomena in Photonic Crystals," *Appl. Phys. Lett.*, Vol. 74, No. 9, pp. 1212-1214, 1999.

[16] J. Witzens, M Loncar, and A. Schere, "Self-Collimation in Planar Photonic Crystals," *IEEE. J. Selected Topics. Quantu. Electrons*, Vol. 8, No. 6, pp. 1246-1257, 2002.

[17] D. W. Prather, S. Shi, D. M. Pustai, C. Chen, S. Venkataraman, A. Sharkawy, G. J. Schneider, and J Murakowski, "Dispersion-Based Optical Routing in Photonic Crystals," *Opt. Lett.*, Vol. 29, No. 1, pp. 50-52, 2004.

[18] S. Olivier, H. Benisty, C. Weisbuch, C. J. M. Smith, T. F. Krauss, R. Houdre, and U. Oesterle, "Improved 60 Bend Transmission of Submicron-Width Waveguides Defined in Two-Dimensional Photonic Crystals," *IEEE J. Lightwave Tech.*, vol. 20, pp. 1198-1203 (2002).

[19] X. Yu and S. Fan, "Bends and Splitters for Self-collimated Beams in Photonic Crystals," *Appl. Phys. Lett.*, vol. 83, pp. 3251-3253 (2003).

[20] T. Matsumoto and T. Baba, "Photonic Crystal k-Vector Superprism," *IEEE J. Lightwave Tech.*, vol . 22, pp. 917-922 (2004).

[21] X. Yu and S. Fan, "Anomalous Reflections at Photonic Crystal Surfaces," *Phys. Rev. E*, vol. 70, pp. 055601-055605, 2004.

[22] Y. Ogawa, Y. Iida, and Y. Omura,"Feasibility Study on Self-Collimated Light-Focusing Device Using 2-D Photonic Crystal with a Parallelogram Lattice," *Ext. Abstract, Int. Conf. on Solid State Devices and Materials*, Tokyo, pp. 584-585, Sept. 2004.

[23] Y. Ogawa, Y. Iida and Y. Omura, "Asymmetrical Transmission of Light Waves In Self-Collimated Light-Focusing Device (LFD) Using 2-D Photonic Crystal with a Parallelogram Lattice," *Tech. Dig. 8th Int. Symp. Contemporary Photonics Technology*, Tokyo, p. 131, 2005.

Yasuhisa Omura received the M. S. degree in applied science in 1975 and the Ph. D. degree in electronics in 1984, both from Kyushu University, Japan. He joined the Musashino Electrical Communications Laboratories, NTT, Tokyo, Japan in 1975. He worked on short-channel CMOS / SIMOX design, LSI processing, and SOI device modeling. In NTT, he contributed to trial demonstrations of CMOS/SIMOX SRAM on the device design and fabrication processing. He moved his position from NTT Atsugi R&D Center to Kansai University, Osaka Prefecture, as a professor after April in 1997, and he is presently working on device physics of ultimately miniaturized MOSFET/SOI, modeling for MOS device design, fluctuation physics and development of silicon photonic devices. He has published 110 regular papers and 110 conference proceedings. He is one of coauthors having published "Device and Circuit Cryogenic Operation for Low Temperature Electronics." (Kluwer Academic Publishers, 2001) and "Fully-Depleted SOI CMOS Circuits and Technology for Ultralow-Power Applications" (Springer, 2006). He has invented various SOI devices–for example-the lateral unidirectional bipolar-type insulated-gate transistor (Lubistor), the high-gain cross-current tetrode (HXT) MOS device, and tunneling-barrier junction (TBJ) SOI MOSFET using SIMOX technology. He has patents for Lubistor in Japan, U.S.A., Canada, United Kingdom, France, Germany, Netherlands, Italy, and Korea. He has 30 patents in Japan and several patents in U. S. A. for SIMOX device technology. He was honored with the Annual Young Researcher Award in 1981 from IEICE, Japan. He has worked on ultra-thin MOSFET/SIMOX device technology over 20 years. Last decade, he demonstrated 0.1- m-gate CMOS/SIMOX devices with a long lifetime in 1991 IEEE IEDM and 1992 Int. Conf. on Solid State Devices and Materials (SSDM). He also demonstrated mesoscopic transport characteristics of 50-nm-channel SOI MOSFETs with 2- or 6-nm-thick silicon film in order to indicate perspectives of future SOI devices in 1997. He served the Technical Committee of IEEE Int. SOI Conf. from 1997 to 1998, and now serves the Program Committee of Int. Symp. on VLSI Technology from 1997 to 2006. In addition, he serves the Program Committee of Int. Workshop on

Low-Temperature Electronics (in Europe) from 1998 to now. From 2007, he shares the Vice Chairperson of IEEE Kansai Chapter. Dr. Omura is a regular member of the Japan Society of Applied Physics (JSAP), the Physical Society of Japan, the Electrochemical Society, a senior member of the Institute of Electrical and Electronics Engineers (IEEE) and a regular member of the Institute of Electronics, Information and Communication Engineers (IEICE).
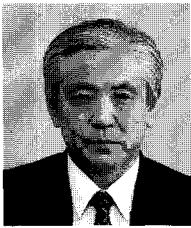
Yukio Iida received the B.E., M.E. and D. Eng. degrees from Kansai University, Osaka, Japan, in 1970, 1972 and 1983, respectively. Since 1979 he has been working at the Department of Electronics, Faculty of Engineering, Kansai University. He was a Research Assistant in 1979, a Lecturer and an Associate Professor. Since 1998 he has been a Professor. He has been engaged in the research of microwave electron tube (Osaka-tube and Gyrotron), wireless blasting system by microwave power, injection locking and multiple oscillation in Gunn, IMPATT and LASER diodes, Spatial network method, FDTD method, electromagnetic field simulation, and silicon microphotonics application including photonic crystal. Dr. Iida is a member of the Institute of Electronics, Information and Communication Engineers (IEICE), Japan, and the IEEE Microwave Theory and Techniques society (IEEE MTT-S).
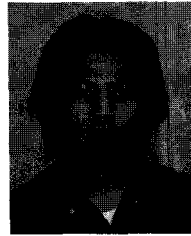
Fumio Urakawa was born in1979 in Nara Pref., Japan, and received the B. S. degree and M. S. degree in Electronics from Kansai University in 2002, and in 2004, respectively. He is presently with ROHM Corporation, Japan.

Yoshifumi Ogawa was born in1979 in Chiba Pref., Japan, and received the B. S. degree and M. S. degree in Electronics from Kansai University in 2003, and in 2005, respectively. He is presently with CANON Corporation, Japan.